文章编号: 1000-324X(2020)12-1315-12 **DOI:** 10.15541/jim20200096

发泡法制备二维材料泡沫体的进展

高 天, 肖庆林, 许晨阳, 王学斌

(南京大学 现代工程与应用科学学院, 固体微结构物理国家重点实验室, 人工微结构科学与技术协同创新中心, 江苏省功能材料设计原理与应用技术重点实验室, 南京 210093)

摘 要: 以石墨烯为代表的二维材料具有优异的本征性质, 例如高表面积和电导率, 但其宏观块体材料的性质仍不理想。这是由于石墨烯片层堆叠损失了有效的表面; 片层之间联结较弱导致接触电阻和热阻增大。原则上二维材料的三维化设计能避免上述问题, 将纳米尺度的优异性质传递到宏观尺度, 获得高表面积、高导电、贯通孔道和优良机械性能的块体材料。二维材料多孔块体可用于电极、吸附剂和弹性体等。发泡法工艺简单、成本低, 是近年来制备二维材料泡沫体的主要方法。本文系统总结了发泡法的基本原理, 综述了石墨烯、氮化硼等二维材料泡沫体的研究进展, 展望了二维材料泡沫体在能源、环境等方面的应用前景。

关 键 词: 二维材料; 发泡法; 石墨烯; 氮化硼; 泡沫材料; 综述

中图分类号: TB321 **文献标识码:** A

Blowing Route to Fabricate Foams of 2D Materials

GAO Tian, XIAO Qinglin, XU Chenyang, WANG Xuebin

(National Laboratory of Solid State Microstructures, Collaborative Innovation Center of Advanced Microstructures, Jiangsu Key Laboratory of Artificial Functional Materials, College of Engineering and Applied Sciences, Nanjing University, Nanjing 210093, China)

Abstract: Graphene, as a representative of two-dimensional (2D) materials, has excellent intrinsic properties such as high specific surface area and conductivity, but its macroscopic bulk behaves poorly owing to severe face-to-face re-stacking and hand-in-hand contact resistance. Three-dimensional (3D) design of 2D materials can deliver the excellent nanoscaled properties to the macroscopic world, to realize the high surface area, conductivity, interconnected pores, and good mechanics of the bulks. It is necessary and highlighted to develop the porous monolith of 2D materials for applications as electrodes, adsorbents, elastomers, *etc*. The blowing route has the advantages of low cost and simple processing, which has been accentually developed to produce the foams of 2D materials for several years. This article introduces the principle of the blowing method, summarizing the recent examples of blown foams of graphene, boron nitride nanosheet, and others. The scientific front about foams of 2D materials is discussed, and the broad applications of the new materials are prospected in energy, environment, *etc*.

Key words: 2D material; blowing method; graphene; boron nitride; foam; review

石墨烯是一种由碳原子通过 sp^2 杂化构成的二维新材料[1], 具有超薄结构和独特物性, 如高载流

收稿日期: 2020-02-29; **收到修改稿日期:** 2020-04-09
基金项目: 青年千人计划; 国家自然科学基金(51972168, 51672124, 21603096); 江苏双创计划
Thousand Talents Plan for Youth; National Natural Science Foundation of China (51972168, 51672124, 21603096); Program for Innovative Talents and Entrepreneur in Jiangsu
作者简介: 高 天(1992–), 男, 博士. E-mail: 1217387634@qq.com
GAO Tian(1992–), male, PhD. E-mail: 1217387634@qq.com
通讯作者: 王学斌, 教授. E-mail: wangxb@nju.edu.cn
WANG Xuebin, professor.E-mail: wangxb@nju.edu.cn

子迁移率、表面积、热导率[2-5]，在电子、储能和催化等领域具有重要的应用前景[6-9]。在石墨烯的宏观块体中，两个相邻片层的面与面之间容易发生 π-π 堆叠，损失表面积；在面内方向，两个相似片层之间通常依靠范德华力联结，接触电阻、热阻较大；此外，片片之间的堆积孔道曲折无序，不利于外来物质的扩散。这三点限制了基于石墨烯的电化学电极等应用性能的提升[10]。

三维石墨烯材料是一种石墨烯块体，与石墨烯粉体、石墨烯薄膜并列，如图 1 所示。在概念上，三维石墨烯是将石墨烯单元连接形成 sp^2 杂化的三维网络。在理论上三维石墨烯可以继承二维纳米材料的本征高比表面积、电导率、热导率等优点。三维网络结构提供的双联通通道为固相网络通道和内部孔道联通形成的空腔通道，前者用于输运电子、声子和力；后者用于传质。三维石墨烯在界面相关应用场景中具有重要意义，包括电极、吸附等[11]。

学者们报导了数种制备三维石墨烯的方法：基于氧化还原石墨烯(RGO)的凝胶化方法(包括体相凝胶化[12-15]、界面凝胶化法[16]、冰模板法[17]、模板/交联剂辅助法[18-19])、基于泡沫镍的化学气相沉积法(CVD)[11,20-21]、基于锌分层效应的热裂解法[22]、生物质热裂解法[23]、发泡法[24]和 3D 打印[25]等。凝胶化方法主要依靠非共价键组装，内部联结较弱；泡沫镍等多孔模板较难循环利用。发泡法工艺简单、成本低、易扩大生产，其产品的固相网络内部联结强、表面积大，是一种极具产业价值的制备方法。除了三维石墨烯，硫化物、双氢氧化物等二维材料多孔块体也是二维材料三维化设计的热门领域[26-28]。

回溯历史，发泡法起源于传统泡沫塑料加工，但在近年开始用于制备二维材料泡沫体。2011~2013 年，王学斌等受吹泡启发，将发泡过程首次引入到二维材料领域，发展了化学发泡法制备石墨烯泡沫体[24]、氮化硼(BN)纳米片泡沫体[29]。随后，LEI[30]和 WANG[31]等利用硝酸盐辅助法制备了石墨烯泡沫体；WANG[32]、ZHAO[33]和 DONG[34]等制备了氮掺杂石墨烯泡沫；DONG[35]、ZHU[36]、WU[37]、CAI[38]和 TAN[39-41]等制备了担载各种功能物质的石墨烯泡沫；LU 等[42]使用铵盐发泡剂制备了氮化碳泡沫；ZHAO 等[43]制备了 BN 泡沫。

本文总结了采用发泡法制备二维材料泡沫体的发泡原理、不同类型泡沫体及其应用，以期阐明未来的发展前景。

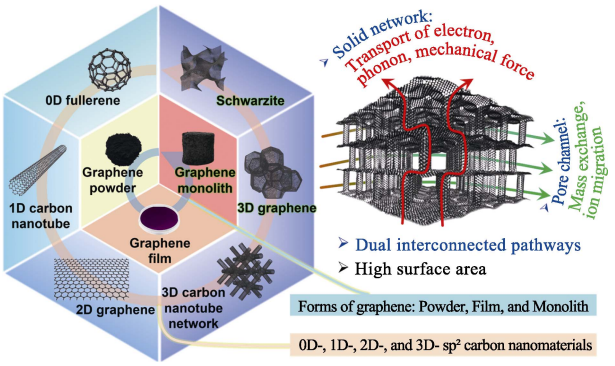

图 1 多种维度的 sp^2 杂化碳纳米材料，石墨烯粉体、薄膜和块体三种形态，以及设计三维石墨烯的理念

Fig. 1 Different-dimensional sp^2-hybrid carbon nanomaterials, graphene forms (powder, film, and monolith), and concept of 3D graphene

1 发泡原理

1.1 发泡流程

发泡过程包括三步(图 2)：①前驱体与发泡剂混合；②在内/外部作用下产生气体源，使气泡成核、长大；③流体泡沫经历稳定化过程最终变成固体泡沫。根据气源不同，发泡法分为化学发泡和物理发泡，前者通过化学反应产生气体，后者则利用沸腾或减压膨胀产生气体。流体泡沫目前基本没有工程用途，它需经历固化、硬化和结晶等稳定化过程。

泡沫的基本单元为气泡，在平衡态时呈多面体形状。气泡由泡壁、筋和交点构成，分别定义为 2、3、4 个气泡的结合部，亦即几何学中的面、棱和点，如图 2 所示。按照 Plateau 定律，3 个泡壁相交于 1 条筋(Plateau 通道)，且倾向对称分布；4 条筋相交于 1 个交点，也倾向对称分布。

1.2 发泡几何学与静力学

泡沫几何学主要研究“干泡沫”的多面体堆砌问题。欧拉定律认为气泡多面体的大多数面应为五边形[44]；Aboav-Weaire 定律认为一个多面体拥有的面数越多，则其相邻多面体的面数就越少[45]。Lewis 定律认为多面体的体积随面数的增加而增加[46]。因此，一个大气泡通常被小气泡所包围。此外，表面张力等静力学因素也影响泡沫的结构。表面能与表面

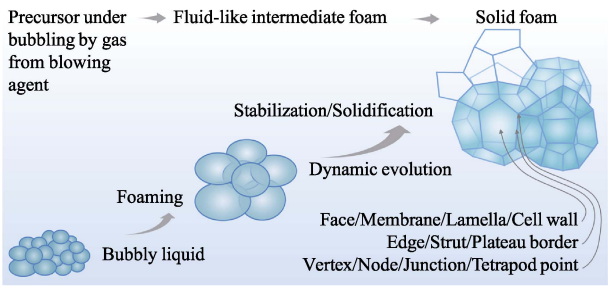

图 2 发泡过程示意图

Fig. 2 Scheme of blowing process

积成正比, 泡沫表面能最小的为密堆多面体, 因为它的表面积最小, 即熟知的 Kelvin 问题。1887 年, Thomson 提出了 Kelvin 结构; 1993 年, Weaire 和 Phelan 构建了 Weaire-Phelan 结构[47], 其表面积比 Kelvin 结构的表面积减少了 0.3%, 如图 3(a,b)所示。堆砌问题的最优方案迄今仍无确切结论。

1.3　发泡动力学与动态学

发泡动力学主要包括: ①气泡的均/异相成核; ②气泡的长大; ③气泡结构的动态演变; ④稳定化过程, 如图 3(c)所示。气泡成核与晶体成核有共通之处, 一旦初生气泡大于临界尺寸, 则倾向于长大; 反之则趋于消失。进一步, 内/外部驱动力驱使气源持续扩散进入气泡, 使气泡长大。

在形核和长大的过程中, 流体泡沫也进行着动态学演化, 包括渗流、熟化、破裂、重排等行为。

(1)渗流是流体泡沫中的流体在表面张力或重力驱动下, 在泡壁和筋内部流动的过程[48]。前者由于不同位置的曲率半径不同, 导致 Lapalce 压力差, 驱使流体自泡壁流向 Plateau 通道。后者由于流体泡沫的质心要降低, 则流体沿着 Plateau 通道自上而下流动。

(2)熟化/粗化是小气泡内的气体向相邻大气泡中扩散的过程, 这是由于小气泡的半径小, 内压大, 与大气泡之间有压差。

(3)液膜破裂。伴随着渗流或流体的挥发, 液膜不断减薄, 当其厚度减薄至黑膜状态时, 楔压会削弱表面张力, 造成液膜破裂, 使两个气泡发生合并。

(4)流体泡沫具有流变特性, 例如典型的 T1 重排。

气泡的成核和生长在很大程度上决定气泡的直径分布, 动态演变亦影响了气泡尺寸、泡壁厚度等。实践发现, 发泡的关键在于发泡剂产气过程与聚合物固化过程之间的匹配。两者的匹配影响了发泡动力学与动态学、流体泡沫的结构, 最终形成固体泡沫。

2　采用发泡法制备二维材料泡沫体

传统发泡工业制造了泡沫塑料[49]、泡沫金属[50]、泡沫陶瓷[51]和泡沫炭[52-54]等民用和特种泡沫。近年来, 学者们拓展了用发泡法制备二维材料泡沫体[24,29]。二维材料泡沫体不仅具有固体泡沫的性质, 又可以呈现二维材料的本征优异特性[28]。基于 B、C、N 和 O 的聚合物种类丰富, 易发泡, 而且在发泡过程中易进行掺杂、包裹/担载金属元素, 发展了多种多样的 B–C–N–O 体系二维材料泡沫体, 包括石墨烯、掺杂和担载型石墨烯、氮化碳和氮化硼等, 如图 4 所示。

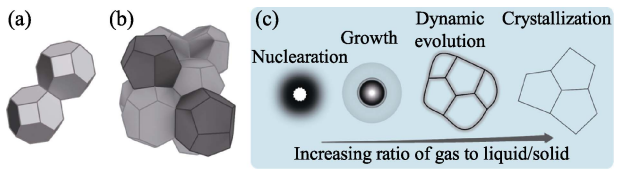

图 3　堆砌的(a)Kelvin 结构和(b)Weaire-Phelan 结构; (c)发泡动力学示意图

Fig. 3　(a) Kelvin structure and (b) Weaire-Phelan structure for honeycomb, (c) scheme of blowing kinetics

2.1　石墨烯类泡沫体

2.1.1　石墨烯泡沫体

2013 年, 王学斌等[24]开拓了化学发泡法制备一种新型三维石墨烯——筋撑石墨烯(strutted graphene, SG), 如图 5(a~d)所示。化学发泡法以糖为碳源, NH_4Cl 为发泡剂, 在加热过程中诱发美拉德反应, 同时 NH_4Cl 分解释放出 NH_3 和 HCl, 使类黑精聚合物发泡。随着气泡膨胀、表面张力渗流和热解反应, 类黑精发泡体的泡壁逐渐减薄, 最终其聚合物泡壁厚度可薄至约 20 nm[55], 如图 5(e~f)所示。类黑精泡沫体经 1350 ℃退火, 转变为 SG。SG 的泡壁为单层或寡层石墨烯薄膜, 如图 5(g~i), 它们附着在石墨筋上。这种筋耦合膜的结构提升了机械弹性, 经 80%的压应变后依然能恢复原状; 同时消除了石墨烯堆叠问题, 实现了 1005 m^2/g 的比表面积。

为了匹配发泡剂产气与聚合物固化两过程, 选择适当发泡剂是控制泡沫结构的重要手段。无残留的发泡剂除了 NH_4Cl (产气温度可持续在 200~270 ℃, 下同), 还可以选择$(NH_4)_2CO_3$(50~80 ℃)、NH_4NO_3 (150~200 ℃)、$(NH_4)_2SO_4$(330~380 ℃)、尿素(170~220 ℃)、草酸(190~220 ℃)和三聚氰胺(270~320 ℃)

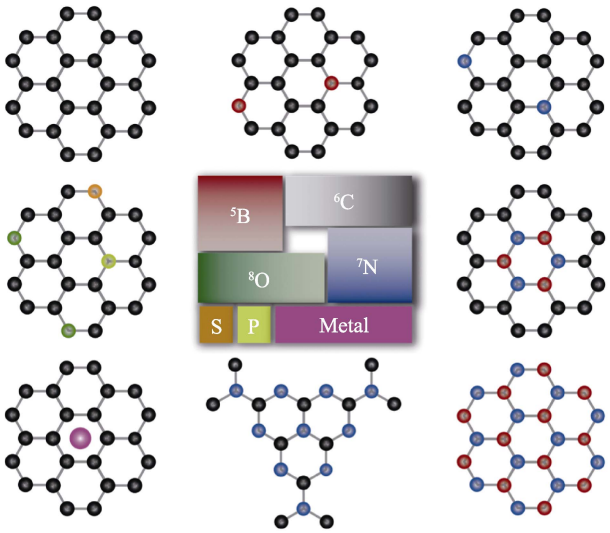

图 4　适合发泡的轻元素 B-C-N-O 体系

Fig. 4　B-C-N-O light-element system suitable for blowing

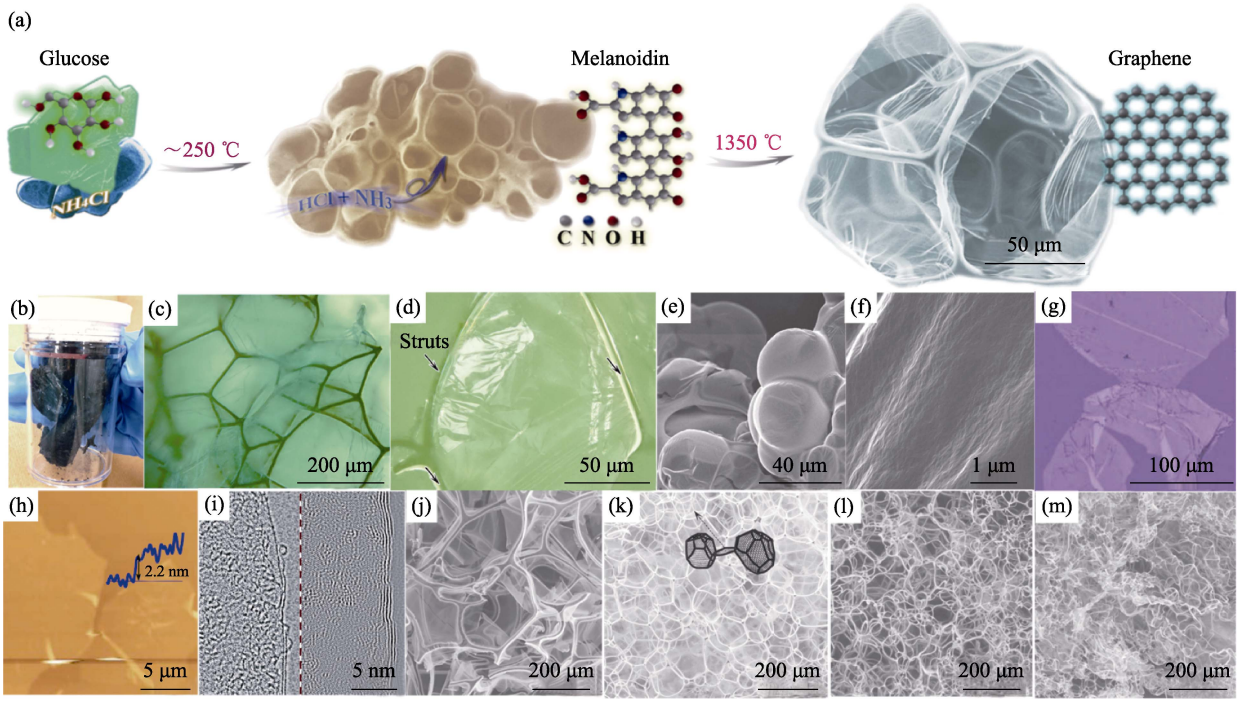

图 5 (a)化学发泡法示意图; (b, c)SG 实物和光学图像; (d)SG 中石墨烯壁和石墨筋的光学图像; (e, f)中间体聚合物泡沫及其泡壁的 SEM 照片; (g)纯化后的石墨烯片层的光学照片; (h)石墨烯片层的 AFM 图像; (i)SG 的 HRTEM 照片; (j~m)分别以 1、4、20、100 ℃/min 加热发泡得到的不同 SG 的 SEM 照片[24,55]

Fig. 5 (a) Scheme of chemical blowing process; (b, c) Photo and optical image of SG; (d) Optical image of a graphene membrane and graphitic struts of SG; (e, f) Scanning electron microscope (SEM) images of intermediate polymeric bubbles and their thin walls; (g) Optical image of a large few-layered graphene membrane taken from SG; (h) Atomic force microscope (AFM) image of an individual graphene membrane; (i) High-resolution transmission electron microscope (HRTEM) images of SG; (j-m) SEM images of strutted graphene grown at heating rates of 1, 4, 20 and 100 ℃/min[24,55]

等。若产气温度高于或低于聚合物固化温度, 则不易发泡。加热速度可以影响产气速度和持续时间, 高速加热时气泡成核多, 则最终泡孔较小; 反之则泡孔较大, 如图 5(j~m)。使用铵盐等无残留发泡剂的报道归纳于表 1 中。

含金属的盐类也可以作为发泡剂。例如, $Fe(NO_3)_3$[30]、$ZnCl_2$[56]、$KHCO_3$[57]和 $Ni(NO_3)_2$[58]分别使葡萄糖、水解淀粉、纤维素、麦芽糖发泡, 用来制备石墨烯泡沫体。从金属元素的角度而言, Na、K 和 Zn 等低沸点金属在发泡过程中对碳有插层/刻蚀作用, 产生活化[59]、分层[22]等效应, 有利于提高表面积。过渡金属元素 Fe、Ni 等, 在加热时可以提高碳的石墨化程度[30,58,60-62], 但需要用强酸洗去这些高沸点金属以获得纯碳泡沫体。

2.1.2 掺杂石墨烯泡沫体

发泡过程要经历聚合物流体状态, 其聚合反应步骤中易于掺入杂原子。N 是常用掺杂元素, 例如吡啶氮可以激活其相邻碳原子成为氧还原催化活性中心[63]。前述铵盐发泡剂就可以在 SG 中掺入 N 元素, N 含量在 300 ℃时为 18at%, 在 1400 ℃时为 0.4at%[55]。由于杂原子在高温下容易流失, 需要提供额外的杂原子源以补偿此损失[64-66], 提高掺杂量。在葡萄糖-NH_4Cl 发泡体系中加入三聚氰胺, 其发泡体在 1100 ℃时含 N 为 8.36at%[65]。此外, 也可进行多元素共掺杂[67-70], 如三聚氰胺分解使季戊四醇三聚氰胺磷酸盐(PMP)发泡, 得到 N–P–O 共掺杂石墨烯泡沫体, 如图 6 所示[67]。

2.1.3 担载型石墨烯泡沫体

在发泡过程中, 若采用含过渡金属盐类作为发泡剂, 则其金属元素可以保留在最终产品中, 构成担载型石墨烯泡沫体。聚乙烯吡咯烷酮(PVP)-$Fe(NO_3)_3$ 体系经历发泡, 可以制得担载 Fe_2O_3 的碳泡沫体[35], 如图 7(a,b)。在葡萄糖-NH_4Cl 体系中分别加入 $CuCl_2$、$CrCl_3$ 和 $Co(NO_3)_2$, 则最终得到担载 Cu[71]、CrN[72]和 Co_2P[36]的碳泡沫体, 如图 7(c,d)。此外, 也可以利用水热法等手段在石墨烯泡沫体上担载功能物质, 例如 SG 担载 NiFeP 超薄纳米片[73], 如图 7(e,g)。使用含金属盐发泡剂的报道汇总于表 2 中。

2.2 类石墨氮化碳泡沫体

LU[42]、GUO[87]、WANG[88]和 TALAPANENI[89]等利用发泡法制备了类石墨氮化碳 g-C_3N_4 纳米片的泡沫体。将三聚氰胺或双氰胺与 NH_4Cl 混合[42,87-88],

表 1　采用发泡法制备的石墨烯泡沫体和掺杂石墨烯泡沫体(使用无残留的铵盐发泡剂)

Table 1　Graphene foams and doped graphene foams fabricated *via* blowing route using residue-free ammonium blowing agents

Precursor	Blowing agent	Heteroatom source	Temperature /℃	Product	SSA /($m^2 \cdot g^{-1}$)	Application	Ref.
Glucose	NH_4Cl	–	1350	Strutted graphene (SG)	1005	Supercapacitor	[24]
Sugar	NH_4Cl	–	1400	Strutted graphene (SG)	710	Supercapacitor	[55]
Glucose	NH_4Cl	–	1000	3D carbon materials (CMs)	170	Li metal battery	[74]
Glucose	$(NH_4)_2CO_3$, citric acid	$(NH_4)_2CO_3$	900	N-doped 3D mesoporous foam	516	Electrocatalysis Thermocatalysis	[64]
Glucose	NH_4Cl, melamine	Melamine	1100	3D N-doped graphene (3DNG) layers	1190	Supercapacitor	[65]
Starch	Urea	Urea	800	N-doped graphitized carbon nanosheets	1947	Supercapacitor	[66]
PMP	Melamine	Melamine, H_3PO_4	1050	N-P-O co-doped monolith carbon aerogel	2668	Supercapacitor Adsorption	[67]
Glucose	Melamine	Melamine, H_3PO_4	1050	P/N co-doped functional exfoliated carbon	1440	Electrocatalysis	[75]
Chitosan	NH_4Cl	NH_4Cl	900	3D hierarchically porous N-doped carbon	1005	Electrocatalysis	[76]
Citric acid	NH_4Cl	NH_4Cl	1000	Hierarchically interconnected N-doped carbon nanosheets (NCNS)	1460	Electrocatalysis	[77]

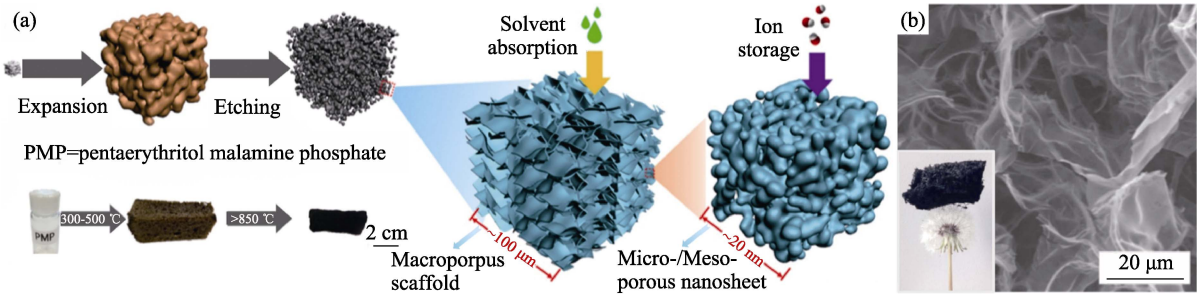

图 6　(a)以三聚氰胺发泡 PMP 过程示意图; (b)N-P-O 共掺杂石墨烯泡沫体的 SEM 照片[67]

Fig. 6　(a) Synthesis scheme of foaming based on PMP precursor; (b) SEM images of N-P-O-co-doped graphene foam[67]

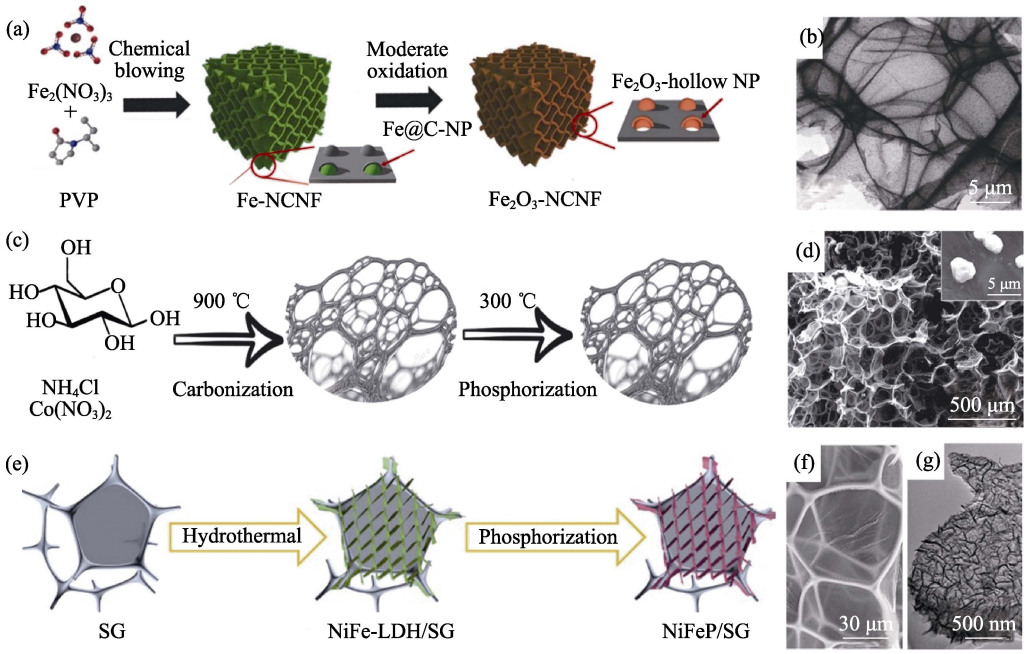

图 7　担载型石墨烯泡沫体制备示意图及其 SEM/HRTEM 照片

Fig. 7　Synthesis schemes and SEM/HRTEM images of loaded graphene foam

(a, b) Fe_2O_3[35]; (c, d) Co_2P[36]; (e, g) NiFeP[73]

表 2 采用发泡法制备石墨烯泡沫体和担载型石墨烯泡沫体(使用含金属元素的盐类作为发泡剂)

Table 2 Pristine and loaded graphene foams fabricated *via* blowing route using metal-contained salt blowing agents

Precursor	Blowing agent of salt	Temperature /℃	Product	SSA /($m^2 \cdot g^{-1}$)	Application	Ref.
Glucose	$Fe(NO_3)_3$	950	Graphene-like carbon nanosheets (GCNs)	220	Electrosorption	[30]
Sucrose	$Zn(NO_3)_2$	1200	Foam-like porous carbon	2340	Supercapacitor	[31]
Hydrolyzed starch	$ZnCl_2$	400	Activated carbon foam with nano-thickness cell walls (ACF-NCW)	926	Supercapacitor	[56]
Cellulose	$KHCO_3$	400	Hierarchically porous carbons (HPCs)	1893	Supercapacitor	[57]
Maltose	$Ni(NO_3)_2$	800	Macroporous graphitic carbon foam (MGCF)	804	Microbial fuel cell	[58]
Sucrose	$Ni(NO_3)_2$	900	Carbon-graphite composite foam	—	Heat dissipation	[60]
Maltose	$Co(NO_3)_2$	900	Graphene-like carbon nanosheets (GCNs)	735	Electrosorption	[61]
Potassium citrate	$C_6H_5K_3O_7$	850	Porous carbon nanosheets (PCNs)	2200	Supercapacitor	[78]
Acrylic-type cation-exchange resin	$Ni(CH_3COO)_2$	850	3D hierarchical porous graphene-like network	1411	Li ion battery	[79]
Artemia cyst shells	$Ni(CH_3COO)_2$	850	N-P-O co-doped 3D graphene	1406	Supercapacitor Electrocatalysis	[33]
Glucose	$Zn(NO_3)_2$	800	N-doped holey graphene	1602	Supercapacitor	[34]
Poly-*o*-phenylenediamine	$Ni(NO_3)_2$	900	3D N-doped graphene (3DNGN)	907	Supercapacitor	[80]
Coal tar pitch	$Mg(CH_3COO)_2$	700	O/N co-doped foam-like porous carbon	1010	Supercapacitor	[81]
EDTA, EG	$Ni(NO_3)_2$	550	3D N-doped carbon nanosheet@carbon nanotube (NCNS@CNT)	375	Supercapacitor	[82]
PVP	$Fe(NO_3)_3$	700	3D N-doped carbon nanosheet frameworks decorated with Fe_2O_3 nanoparticles (Fe_2O_3-NCNF)	306	Li ion battery	[35]
Glucose	$Co(NO_3)_2$	900	CoO@Co/N-doped carbon (CoO@Co/N-C)	551	Electrocatalysis	[36]
Glucose	$Sb(CH_3COO)_3$, NH_4Cl	950	Sb/C composite material	—	Na ion battery	[37]
Glucose	$(NH_4)_2MoS_4$, NH_4Cl	1000	MoS_2/3D graphene structure (MoS_2-G)	—	Electrocatalysis	[38]
PVP	$Fe(NO_3)_3$	800	3D foam-like graphenic carbon scaffold incorporated with FeP nanoparticles (FeP@FGCS)	159	K ion battery	[39]
PVP	$Fe(NO_3)_3$	900	Fe_xO nanospheres anchored on 3D N-doped few-layer graphene framework (Fe_xO@NFLG)	239	K ion battery	[40]
PVP	$Fe(NO_3)_3$	750	3D N-doped graphenic framework coupled with Fe_3C@porous graphite carbon core-shell structures (Fe_3C@PGC-NGF)	238	K ion battery	[41]
Glucose	$CuCl_2$, NH_4Cl	900	Cu/graphene composite	—	Catalysis	[71]
Glucose	$CrCl_3$	1050	Cr^{6+}@graphene	—	Electrocatalysis	[72]
Gelatin	$Fe(NO_3)_3$	500	Fe_2O_3@N-doped carbon foam	418	Supercapacitor Li ion battery	[83]
Polydopamine	$Co(NO_3)_2$	900	Metal and nitrogen co-doped carbon (M/N-C)	276	Electrocatalysis	[84]
Wheat flour	$Co(NO_3)_2$	800	N,S- doped hierarchically porous carbon with core-shell Co@C nanoparticles (Co-N-S-PC)	734	Catalysis	[85]
Glucose	$Ni(NO_3)_2$	650	Graphene-like foam/NiO composite (GLF/NiO)	323	Supercapacitor	[86]

在 550~600 ℃下共热, 则 NH_4Cl 分解产气可使 Melem 等中间体发泡, 最终得到 g-C_3N_4 泡沫体, 如图 8 所示。g-C_3N_4 泡沫体可以增强光催化产氢[42,88]和降解有机污染物[87-88]。

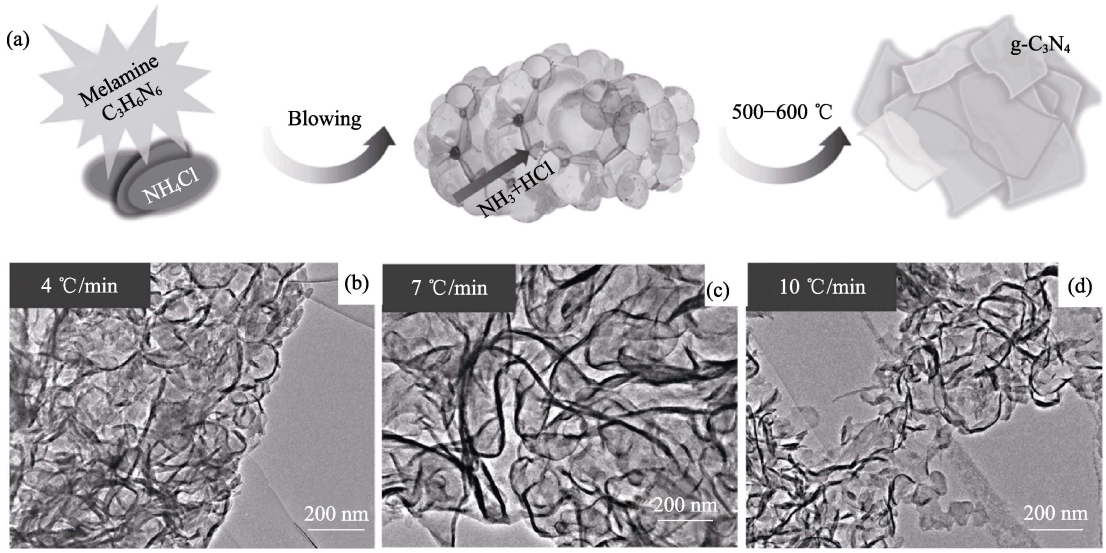

图 8　g-C_3N_4 泡沫体的(a)合成示意图及(b~d)不同加热速率下发泡所获得样品的 TEM 照片[87]

Fig. 8　(a) Synthesis scheme and (b-d) TEM images of 3D strutted g-C_3N_4 foam heated at different rates[87]

2.3　氮化硼泡沫体及硼碳氮杂化泡沫体

六方氮化硼(BN)具有与石墨类似的强层内 σ 键和弱层间范德华力, 与石墨有类似的热学和力学性质。由于异原子成键, BN 具有部分离子性, 其光学、电学性质与石墨截然相反, 如宽带隙、绝缘。BN 有独特的用途, 例如导热、润滑、绝缘、深紫外发光、中子吸收和抗癌等[90-94]。

王学斌等[29]通过加热氨硼烷(AB)使之自发泡, 制备了 BN 泡沫体, 如图 9(a~e)所示。在加热过程中, AB 聚合为聚氨硼烷(PAB)、聚亚氨硼烷(PIB), 并释放出 H_2, H_2 恰能使 PAB 和 PIB 发泡, 最终在 1200 ℃下得到 BN 泡沫体, 经进一步纯化可以获得 BN 纳米片。作为改良, 对 AB 进行预处理[95-96], 可以提高产品表面积。外加发泡剂可以使发泡过程更加可控, 例如在 AB 中添加硫脲或氨基硫脲发泡剂[43]。考虑到 AB 成本较高, WENG 等[97]探索了更低成本的前驱体。将硼酸–聚环氧乙烷(PEO)在 NH_3 气氛下加热, PEO 为发泡剂, 最终得到多孔 BN, 如图 9(f~h)。其它相关体系为氧化硼–盐酸胍[98]、氟硼酸铵–叠氮化钠[99]、硼酸–氰胺类物质[100-101]、硼酸–甲醛–双氰胺[102]和硼酸–尿素[103-104]等。

鉴于 BN 和石墨互补的电学和光学性质, BC_xN 有望实现带隙调变[105]。在上述 AB 自发泡过程中, 通入乙醇气氛, 可以获得 C_x-BN 杂化纳米片的发泡体, x 可在 0.3~0.7 之间调变, 具有半导体特性[29]。

2.4　氧化物纳米片泡沫体

利用金属盐类发泡剂进行发泡时, 如果将惰性气氛调整为氧化性气氛, 则在合适条件下可得到氧化物纳米片泡沫体[32,35,106]。在陶瓷浆料的传统物理发泡过程中, 往往要加入表面活性剂降低发泡难度[107]。使用金属盐类发泡剂使碳基聚合物发泡, 则聚合物泡沫起到模板的作用, 引导金属元素的分布, 最后经氧化转化为氧化物的筋、膜, 构成氧化物泡沫体, 例如 Mn_3O_4[32]、Fe_2O_3[32,35]、MgO[106]、MnO_2[107]、V_2O_5[107]和 MoO_3[107]等。

3　二维材料泡沫体的应用

二维材料泡沫体兼备二维材料和泡沫结构的优点, 是一种有潜力的新材料, 不仅可以用作结构支撑材料, 也可用作多领域功能材料, 如图 10 所示。

在力学方面, 泡沫体是一种轻质支撑材料, 如同自然界演化出的骨头和树木, 可用作包装、填充和漂浮等[29,96,108-109]。石墨烯泡沫体可以支撑自身重量 50000 倍的物体[17]。三维网络结构可以经 99%应变后表现出良好的回弹性, 可循环上千次[110]。石墨烯泡沫体还可以吸收冲击能量[17,110]。低杨氏模量的泡沫体可用于压敏传感[111]。

在热学方面, 石墨烯泡沫体和 BN 泡沫体在热控领域应用广泛。它们可以作为三维化填料用于导热增强复合材料, 以减小填料-填料的界面热阻。石墨烯泡沫体还可以用作相变蓄热材料的填料[112]。BN 泡沫体可以用于增强聚合物基复合材料的热导率[113-118], 用于电子封装等方面。

在吸附相关方面, 石墨烯泡沫体和 BN 泡沫体可以捕获 CO_2[119,120]、储氢[120,121]、储甲烷[120]、吸附有机污染物[122-125]、油水分离[126-128]、吸附重金属离子[99,102]和气敏传感[21]。BN 泡沫体吸附能力高, 而且化学稳定性强, 循环性能优异。

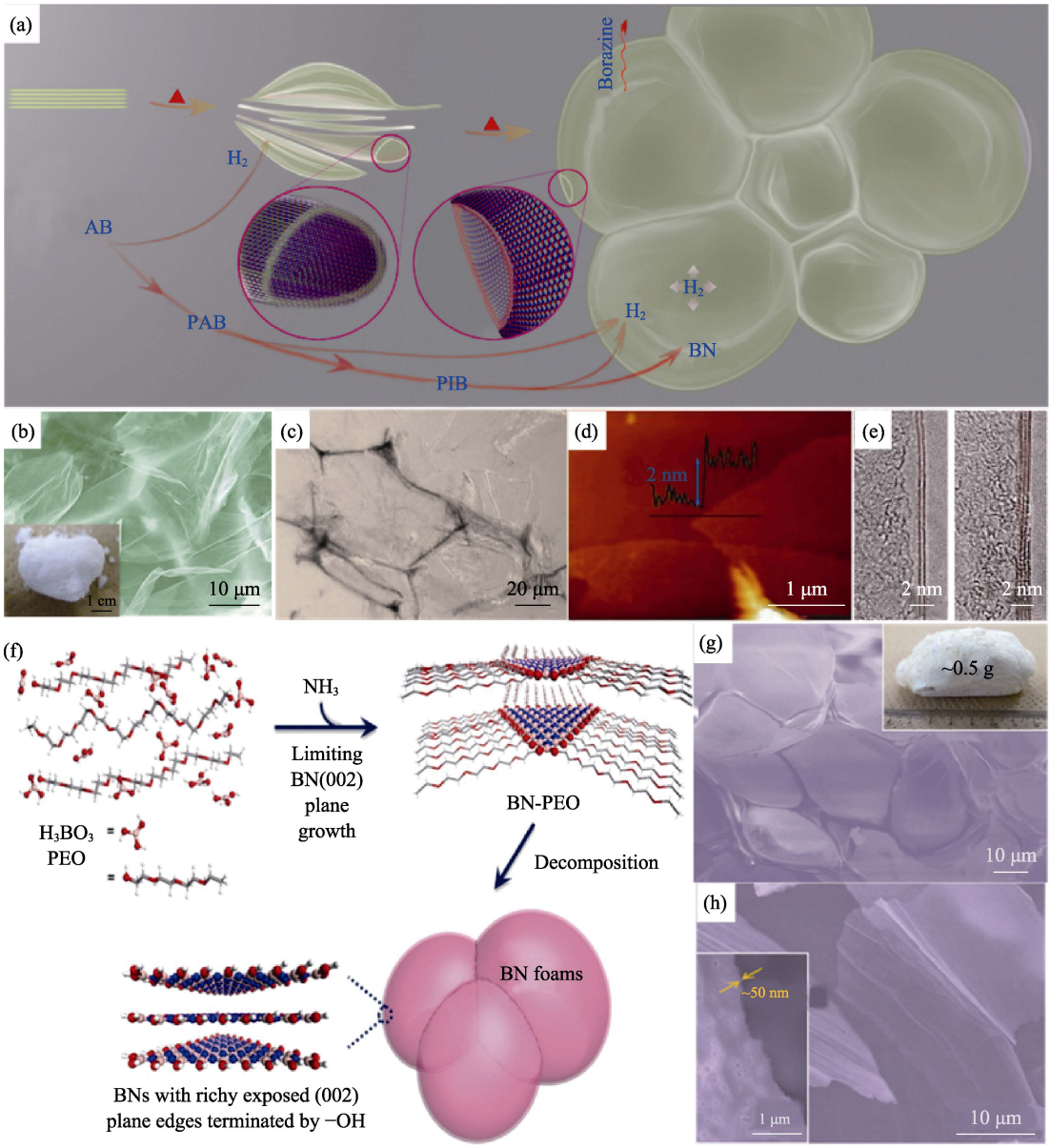

图 9 氨硼烷(AB)自发泡法制备 BN 泡沫体: (a)示意图, (b)SEM 照片, (c)光学照片, (d)AFM 和 HRTEM 图像[29]; 硼酸-PEO 体系发泡制备 BN 泡沫体: (f)示意图, (g, h)SEM 照片[97]

Fig. 9 (a) Synthesis scheme, (b) SEM, (c) optical, (d) AFM and (e) HRTEM images of BN foam by foaming of AB[29]; (f) Synthesis scheme and (g, h) SEM images of BN foam using boric acid and PEO[97]

在电化学方面, 石墨烯泡沫体可用作先进的电化学多孔电极。石墨烯泡沫体适用于超级电容器, 其高表面积有助于实现高容量; 同时高电导、内部孔腔网络有助于实现高功率[129-132]。掺杂和担载型石墨烯泡沫体可以用于电化学储能和催化, 包括赝电容器[133]、锂离子电池[35,79,83]、钠离子电池[37]、钾离子电池[39-41]、燃料电池[33,64,75,84]、微生物燃料电池[58]和电催化分解水[36,73,84]等方面。

在电学方面, 石墨烯泡沫体可用作多孔集流体, 代替泡沫镍等, 以改善电流分布[134]。它具有憎水性, 可以用作防水透气气体电极。石墨烯基泡沫体还可以吸声、吸波、屏蔽电磁波和吸收散乱电子[135]。

4 结束语

二维材料的三维化设计是二维材料宏观块体材料发展的必由之路。二维材料泡沫体具有优良的机械特性, 同时提供了双联通(固相、空腔)的网络结构、高比表面积, 对于界面相关的应用意义重大。发泡法是一种低成本、可工业化的工艺, 可以制备先进的二维材料泡沫体, 但本领域仍有一些亟需研究的难点和发展前沿:

1)可控性是发泡制备工艺的难点。由于发泡体系的复杂性, 目前尚难以精确控制泡孔的尺寸和均匀性。此外, 开发混合发泡剂也是一个新的研究方向。

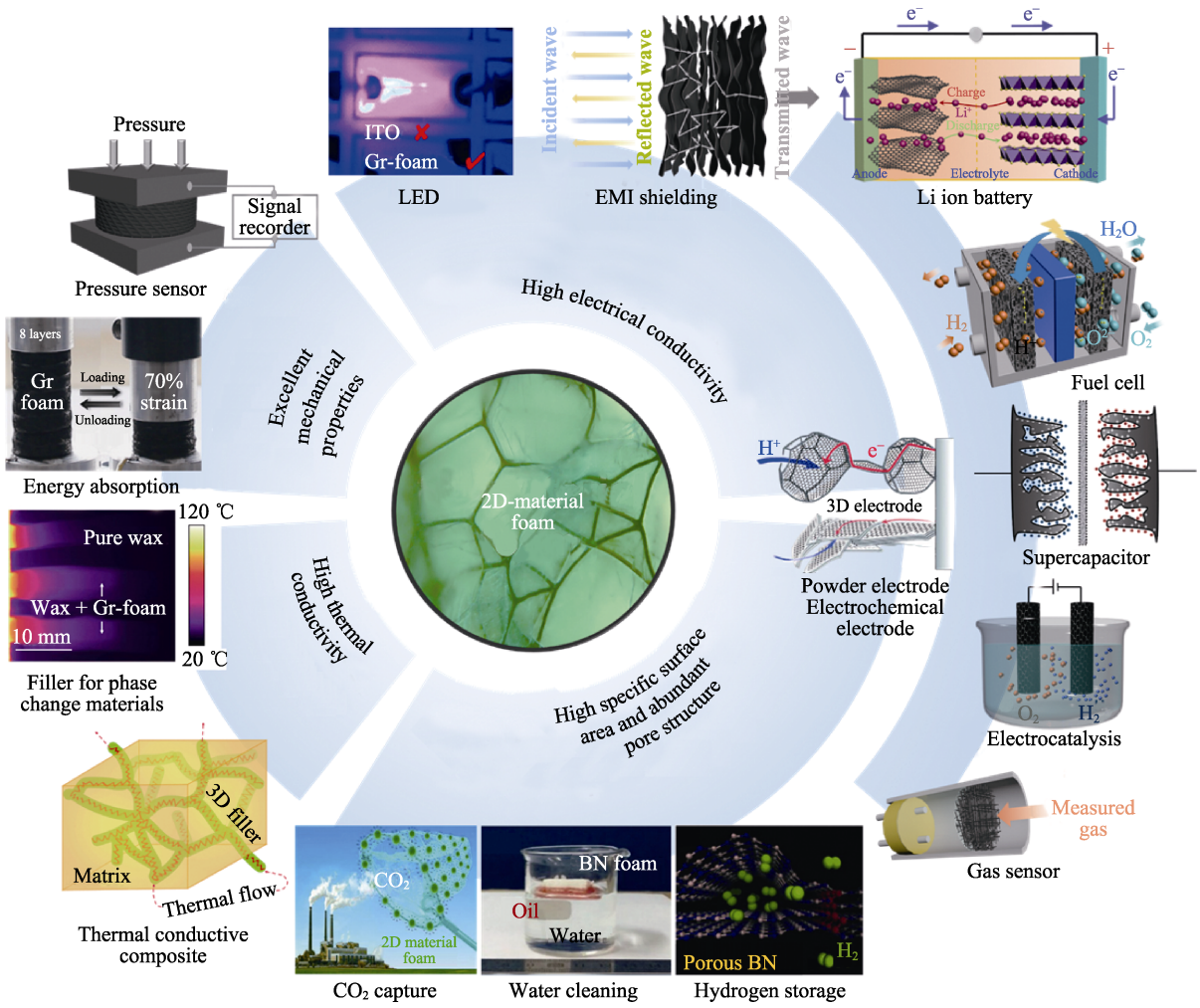

图 10　基于二维材料泡沫体的应用

Fig. 10　Abundant applications based on 2D-material foams

2)发泡法目前集中于 B–C–N–O 轻元素体系，极少用于其它二维材料泡沫体。有待大力发展过渡金属硫化物、层状双氢氧化物和过渡金属碳氮化物的泡沫体。

3)设计制备新型结构的泡沫体是新材料的发展重点，例如，负泊松比的挤缩泡沫体、分等级多级孔泡沫体和负曲率曲面的泡沫体等。

期待通过完善发泡理论，探索发泡体系并提高工艺可控性，发展多种二维材料泡沫体新材料；解析二维材料泡沫体的构效关系，开发其在多学科多领域的丰富应用。

参考文献:

[1] LIAO L, PENG H, LIU Z. Chemistry makes graphene beyond graphene. *J. Am. Chem. Soc.*, 2014, **136(35):** 12194–12200.

[2] HUANG X, QI X, BOEY F, *et al.* Graphene-based composites. *Chem. Soc. Rev.*, 2012, **41(2):** 666–686.

[3] NAIR R R, BLAKE P, GRIGORENKO A N, *et al.* Fine structure constant defines visual transparency of graphene. *Science*, 2008, **320(5881):** 1308.

[4] BALANDIN A A, GHOSH S, BAO W, *et al.* Superior thermal conductivity of single-layer graphene. *Nano Lett.*, 2008, **8(3):** 902–907.

[5] BOLOTIN K I, SIKES K J, JIANG Z, *et al.* Ultrahigh electron mobility in suspended graphene. *Solid State Commun.*, 2008, **146(9/10):** 351–355.

[6] LENG K, ZHANG F, ZHANG L, *et al.* Graphene-based Li-ion hybrid supercapacitors with ultrahigh performance. *Nano Res.*, 2013, **6(8):** 581–592.

[7] XIE G, ZHANG K, GUO B, *et al.* Graphene-based materials for hydrogen generation from light-driven water splitting. *Adv. Mater.*, 2013, **25(28):** 3820–3839.

[8] HOU J, SHAO Y, ELLIS M W, *et al.* Graphene-based electrochemical energy conversion and storage: fuel cells, supercapacitors and lithium ion batteries. *Phys. Chem. Chem. Phys.*, 2011, **13(34):** 15384–15402.

[9] BROWNSON D A C, KAMPOURIS D K, BANKS C E. An overview of graphene in energy production and storage applications. *J. Power Sources*, 2011, **196(11):** 4873–4885.

[10] LU B, LI T, ZHAO H, *et al.* Graphene-based composite materials beneficial to wound healing. *Nanoscale*, 2012, **4(9):** 2978–2982.

[11] CHEN Z, REN W, GAO L, *et al.* Three-dimensional flexible and conductive interconnected graphene networks grown by chemical vapour deposition. *Nat. Mater.*, 2011, **10(6):** 424–428.

[12] LI D, MULLER M B, GILJE S, *et al.* Processable aqueous dispersions of graphene nanosheets. *Nat. Nanotechnol.*, 2008, **3(2):** 101–105.

[13] XU Y, SHENG K, LI C, *et al*. Self-assembled graphene hydrogel *via* a one-step hydrothermal process. *ACS Nano*, 2010, **4(7):** 4324–4330.
[14] XU Y, LIN Z, HUANG X, *et al.* Functionalized graphene hydrogel-based high-performance supercapacitors. *Adv. Mater.*, 2013, **25(40):** 5779–5784.
[15] MAO S, LU G, CHEN J. Three-dimensional graphene-based composites for energy applications. *Nanoscale*, 2015, **7(16):** 6924–6943.
[16] YANG X, QIU L, CHENG C, *et al*. Ordered gelation of chemically converted graphene for next-generation electroconductive hydrogel films. *Angew. Chem. Int. Ed.*, 2011, **50(32):** 7325–7328.
[17] QIU L, LIU J, CHANG S, *et al.* Biomimetic superelastic graphene-based cellular monoliths. *Nat. Commun.*, 2012, **3:** 1241.
[18] TANG Z, SHEN S, ZHUANG J, *et al*. Noble-metal-promoted three-dimensional macroassembly of single-layered graphene oxide. *Angew. Chem. Int. Ed.*, 2010, **122(27):** 4707–4711.
[19] XU Y, WU Q, SUN Y, *et al.* Three-dimensional self-assembly of graphene oxide and DNA into multifunctional hydrogels. *ACS Nano*, 2010, **4(12):** 7358–7362.
[20] CAO X, SHI Y, SHI W, *et al.* Preparation of novel 3D graphene networks for supercapacitor applications. *Small*, 2011, **7(22):** 3163–3168.
[21] YAVARI F, CHEN Z, THOMAS A V, *et al.* High sensitivity gas detection using a macroscopic three-dimensional graphene foam network. *Sci. Rep.*, 2011, **1:**166.
[22] JIANG X, LI R, HU M. *et al*. Zinc-tiered synthesis of 3D graphene for monolithic electrodes. *Adv. Mater.*, 2019, **31(25):** e1901186.
[23] GAO T, XU C, LI R, *et al*. Biomass-derived carbon paper to sandwich magnetite anode for long-life Li-ion battery. *ACS Nano*, 2019, **13(10):** 11901–11911.
[24] WANG X, ZHANG Y, ZHI C, *et al.* Three-dimensional strutted graphene grown by substrate-free sugar blowing for high-power-density supercapacitors. *Nat. Commun.*, 2013, **4(4):** 2905.
[25] JIANG Y, XU Z, HUANG T, *et al*. Direct 3D printing of ultralight graphene oxide aerogel microlattices. *Adv. Funct. Mater.*, 2018, **28(16):** 1707024.
[26] SHEHZAD K, XU Y, GAO C, *et al.* Three-dimensional macro-structures of two-dimensional nanomaterials. *Chem. Soc. Rev.*, 2016, **45(20):** 5541–5588.
[27] ITO Y, TANABE Y, QIU H J, *et al.* High-quality three-dimensional nanoporous graphene. *Angew. Chem. Int. Ed.*, 2014, **126(19):** 4922–4926.
[28] QIU L, HE Z, LI D. Multifunctional cellular materials based on 2D nanomaterials: prospects and challenges. *Adv. Mater.*, 2017, **30(4):** 1704850.
[29] WANG X, ZHI C, LI L, *et al.* "Chemical blowing" of thin-walled bubbles: high-throughput fabrication of large-area, few-layered BN and C(*x*)-BN nanosheets. *Adv. Mater.*, 2011, **23(35):** 4072–4076.
[30] LEI H, YAN T, WANG H, *et al.* Graphene-like carbon nanosheets prepared by a Fe-catalyzed glucose-blowing method for capacitive deionization. *J. Mater. Chem. A*, 2015, **3(11):** 5934–5941.
[31] WANG C, O'CONNELL M J, CHAN C K. Facile one-pot synthesis of highly porous carbon foams for high-performance supercapacitors using template-free direct pyrolysis. *ACS Appl. Mater. Interfaces*, 2015, **7(16):** 8952–8960.
[32] WANG D, ZHOU W, ZHANG R, *et al.* Mass production of large-sized, nonlayered 2D nanosheets: their directed synthesis by a rapid "gel-blowing" strategy, and applications in Li/Na storage and catalysis. *Adv. Mater.*, 2018, **30(43):** 1803569.
[33] ZHAO Y, HUANG S, XIA M, *et al.* N-P-O co-doped high performance 3D graphene prepared through red phosphorous-assisted "cutting-thin" technique: a universal synthesis and multifunctional applications. *Nano Energy*, 2016, **28:** 346–355.
[34] DONG X, HU N, WEI L, *et al.* A new strategy to prepare N-doped holey graphene for high-volumetric supercapacitors. *J. Mater. Chem. A*, 2016, **4(25):** 9739–9743.
[35] DONG Y, YU M, WANG Z, *et al.* A top-down strategy toward 3D carbon nanosheet frameworks decorated with hollow nanostructures for superior lithium storage. *Adv. Funct. Mater.*, 2016, **26(42):** 7590–7598.
[36] ZHU C, FU S, XU B, *et al.* Sugar blowing-induced porous cobalt phosphide/nitrogen-doped carbon nanostructures with enhanced electrochemical oxidation performance toward water and other small molecules. *Small*, 2017, **13(33):** 1700796.
[37] WU Z, JOHANNESSEN B, ZHANG W, *et al. In situ* incorporation of nanostructured antimony in an N-doped carbon matrix for advanced sodium-ion batteries. *J. Mater. Chem. A*, 2019, **7(20):** 12842–12850.
[38] CAI L, LIN Z, WANG M, *et al*. Improved interfacial H_2O supply by surface hydroxyl groups for enhanced alkaline hydrogen evolution. *J. Mater. Chem. A*, 2017, **5(46):** 24091–24097.
[39] TAN Q, ZHAO W, HAN K, *et al*. The multi-yolk/shell structure of FeP@foam-like graphenic scaffolds: strong P-C bonds and electrolyte- and binder-optimization boost potassium storage. *J. Mater. Chem. A*, 2019, **7(26):** 15673–15682.
[40] TAN Q, LI P, HAN K, *et al*. Chemically bubbled hollow Fe_xO nanospheres anchored on 3D N-doped few-layer graphene architecture as a performance-enhanced anode material for potassium-ion batteries. *J. Mater. Chem. A*, 2019, **7(2):** 744–754.
[41] HAN K, LIU Z, LI P, *et al.* High-throughput fabrication of 3D N-doped graphenic framework coupled with Fe_3C@porous graphite carbon for ultrastable potassium ion storage. *Energy Storage Mater.*, 2019, **22:** 185–193.
[42] LU X, XU K, CHEN P, *et al.* Facile one step method realizing scalable production of g-C_3N_4 nanosheets and study of their photocatalytic H_2 evolution activity. *J. Mater. Chem. A*, 2014, **2(44):** 18924–18928.
[43] ZHAO H, SONG X, ZENG H. 3D white graphene foam scavengers: vesicant-assisted foaming boosts the gram-level yield and forms hierarchical pores for superstrong pollutant removal applications. *NPG Asia Mater.*, 2015, **7(3):** e168.
[44] LAKATOS I. Proofs and refutations: the logic of mathematical discovery, 4th ed. Cambridge: Cambridge University Press, 2015, 1–183.
[45] WEAIRE D. Some remarks on the arrangement of grains in a polycrystal. *Metallography*, 1974, **7(2):** 157–160.
[46] RIVIER N. Recent results on the ideal structure of glasses. *J. Physique Colloques*, 1982, **43(C9):** 91–95.
[47] WEAIRE D, PHELAN R. A counter-example to Kelvin's conjecture on minimal surfaces. *Philos. Mag. Lett.*, 1994, **69(2):** 107–110.
[48] 黄晋, 孙其诚. 液态泡沫渗流的机理研究进展. 力学进展, 2007, **37(2):** 269–278.
[49] ZHOU C, YANG K, WANG K, *et al.* Combination of fused deposition modeling and gas foaming technique to fabricated hierarchical macro/microporous polymer scaffolds. *Mater. Des.*, 2016, **109:** 415–424.
[50] BANHART J. Light-metal foams-history of innovation and technological challenges. *Adv. Eng. Mater.*, 2013, **15(3):** 82–111.
[51] STUDART A R, GONZENBACH U T, TERVOORT E, *et al.* Processing routes to macroporous ceramics: a review. *J. Am. Ceram. Soc.*, 2006, **89(6):** 1771–1789.
[52] INAGAKI M, QIU J, GUO Q. Carbon foam: preparation and application. *Carbon*, 2015, **87:** 128–152.
[53] LIU M, GAN L, ZHAO F, *et al.* Carbon foams with high compressive strength derived from polyarylacetylene resin. *Carbon*, 2007, **45(15):** 3055–3057.
[54] CHEN S, HE G, HU H, *et al.* Elastic carbon foam *via* direct carbonization of polymer foam for flexible electrodes and organic chemical absorption. *Energy Environ. Sci.*, 2013, **6(8):** 2435–2439.
[55] JIANG X, WANG X, DAI P, *et al.* High-throughput fabrication

of strutted graphene by ammonium-assisted chemical blowing for high-performance supercapacitors. *Nano Energy*, 2015, **16:** 81–90.

[56] LEI H, CHEN D, HUO J. Blowing and *in-situ* activation of carbonaceous "lather" from starch: preparation and potential application. *Mater. Des.*, 2016, **92:** 362–370.

[57] DENG J, XIONG T, XU F, *et al.* Inspired by bread leavening: one-pot synthesis of hierarchically porous carbon for supercapacitors. *Green Chem.*, 2015, **17(7):** 4053–4060.

[58] JIANG H, YANG L, DENG W, *et al.* Macroporous graphitic carbon foam decorated with polydopamine as a high-performance anode for microbial fuel cell. *J. Power Sources*, 2017, **363:** 27–33.

[59] ZHU Y, MURALI S, STOLLER M D, *et al.* Carbon-based supercapacitors produced by activation of graphene. *Science*, 2011, **332(6037):** 1537–1541.

[60] JANA P, BARRIO E P D, FIERRO V, *et al.* Design of carbon foams for seasonal solar thermal energy storage. *Carbon*, 2016, **109:** 771–787.

[61] JIANG H, WANG S, DENG W, *et al.* Graphene-like carbon nanosheets as a new electrode material for electrochemical determination of hydroquinone and catechol. *Talanta*, 2017, **164:** 300–306.

[62] LI Y, LI Z, SHEN P. Simultaneous formation of ultrahigh surface area and three-dimensional hierarchical porous graphene-like networks for fast and highly stable supercapacitors. *Adv. Mater.*, 2013, **25(17):** 2474–2480.

[63] GUO D, SHIBUYA R, AKIBA C, *et al.* Active sites of nitrogen-doped carbon materials for oxygen reduction reaction clarified using model catalysts. *Science*, 2016, **351(6271):** 361–365.

[64] BA H, LIU Y, TRUONG-PHUOC L, *et al.* N-doped food-grade-derived 3D mesoporous foams as metal-free systems for catalysis. *ACS Catal.*, 2016, **6(3):** 1408–1419.

[65] HAO J, SHU D, GUO S, *et al.* Preparation of three-dimensional nitrogen-doped graphene layers by gas foaming method and its electrochemical capactive behavior. *Electrochim. Acta*, 2016, **193:** 293–301.

[66] CHANG B, YIN H, ZHANG X, *et al.* Chemical blowing strategy synthesis of nitrogen-rich porous graphitized carbon nanosheets: morphology, pore structure and supercapacitor application. *Chem. Eng. J.*, 2017, **312:** 191–203.

[67] QI F, XIA Z, JIN J, *et al.* Chemical foaming coupled self-etching: a multiscale processing strategy for ultrahigh-surface-area carbon aerogels. *ACS Appl. Mater. Interfaces*, 2018, **10(3):** 2819–2827.

[68] ZHENG Y, JIAO Y, GE L, *et al.* Two-step boron and nitrogen doping in graphene for enhanced synergistic catalysis. *Angew. Chem. Int. Ed.*, 2013, **52(11):** 3110–3116.

[69] ZHAO Y, YANG L, CHEN S, *et al*. Can boron and nitrogen co-doping improve oxygen reduction reaction activity of carbon nanotubes? *J. Am. Chem. Soc.*, 2013, **135(4):** 1201–1204.

[70] JIAO Y, ZHENG Y, DAVEY K, *et al.* Activity origin and catalyst design principles for electrocatalytic hydrogen evolution on heteroatom-doped graphene. *Nat. Energy*, 2016, **1(10):** 16130.

[71] JIN L, HE G, XUE J, *et al.* Cu/graphene with high catalytic activity prepared by glucose blowing for reduction of *p*-nitrophenol. *J. Cleaner Prod.*, 2017, **161:** 655–662.

[72] YAO Y, XU Z, CHENG F, *et al.* Unlocking the potential of graphene for water oxidation using an orbital hybridization strategy. *Energy Environ. Sci.*, 2018, **11(2):** 407–416.

[73] LI R, WANG B, GAO T, *et al*. Monolithic electrode integrated of ultrathin NiFeP on 3D strutted graphene for bifunctionally efficient overall water splitting. *Nano Energy*, 2019, **58:** 870–876.

[74] XU Y, WANG L, JIA W, *et al*. Three-dimensional carbon material as stable host for dendrite-free lithium metal anodes. *Electrochim. Acta*, 2019, **301:** 251–257.

[75] JIN J, GU L, JIANG L, *et al.* A direct phase separation approach synthesis of hierarchically porous functional carbon as an advanced electrocatalyst for oxygen reduction reaction. *Carbon*, 2016, **109:** 306–313.

[76] WANG Y, HAO J, YU J, *et al*. Hierarchically porous N-doped carbon derived from biomass as oxygen reduction electrocatalyst for high-performance Al-air battery. *J. Energy Chem.*, 2020, **45:** 119–125.

[77] WANG H, YI Q, GAO L, *et al.* Hierarchically interconnected nitrogen-doped carbon nanosheets for an efficient hydrogen evolution reaction. *Nanoscale*, 2017, **9(42):** 16342–16348.

[78] SEVILLA M, FUERTES A B. Direct synthesis of highly porous interconnected carbon nanosheets and their application as high-performance supercapacitors. *ACS Nano*, 2014, **8(5):** 5069–5078.

[79] LI Y, ZHANG H, SHEN P. Ultrasmall metal oxide nanoparticles anchored on three-dimensional hierarchical porous gaphene-like networks as anode for high-performance lithium ion batteries. *Nano Energy*, 2015, **13:** 563–572.

[80] DENG W, ZHANG Y, TAN Y, *et al.* Three-dimensional nitrogen-doped graphene derived from poly-o-phenylenediamine for high-performance supercapacitors. *J. Electroanal. Chem.*, 2017, **787:** 103–109.

[81] SHAO J, MA F, WU G, *et al.* Facile preparation of 3D nanostructured O/N co-doped porous carbon constructed by interconnected carbon nanosheets for excellent-performance supercapacitors. *Electrochim. Acta*, 2016, **222:** 793–805.

[82] ZHOU W, DU Y, ZENG J, *et al.* A modified "gel-blowing" strategy toward the one-step mass production of a 3D N-doped carbon nanosheet@carbon nanotube hybrid network for supercapacitors. *Nanoscale*, 2019, **11(16):** 7624–7633.

[83] LI J, WANG N, DENG J, *et al.* Flexible metal-templated fabrication of mesoporous onion-like carbon and Fe_2O_3@N-doped carbon foam for electrochemical energy storage. *J. Mater. Chem. A*, 2018, **6(27):** 13012–13020.

[84] LI B, CHEN Y, GE X, *et al.* Mussel-inspired one-pot synthesis of transition metal and nitrogen co-doped carbon (M/N-C) as efficient oxygen catalysts for Zn-air batteries. *Nanoscale*, 2016, **8(9):** 5067–5075.

[85] TIAN W, ZHANG H, QIAN Z, *et al.* Bread-making synthesis of hierarchically Co@C nanoarchitecture in heteroatom doped porous carbons for oxidative degradation of emerging contaminants. *Appl. Catal. B*, 2018, **225:** 76–83.

[86] HE C, JIANG Y, ZHANG X, *et al.* A simple glucose-blowing approach to graphene-like foam/NiO composites for asymmetric supercapacitors. *Energy Technol.*, 2019**:** 1900923.

[87] GUO Q, ZHANG Y, ZHANG H, *et al.* 3D foam strutted graphene carbon nitride with highly stable optoelectronic properties. *Adv. Funct. Mater.*, 2017, **27(42):** 1703711.

[88] WANG H, WU Y, FENG M, *et al.* Visible-light-driven removal of tetracycline antibiotics and reclamation of hydrogen energy from natural water matrices and wastewater by polymeric carbon nitride foam. *Water. Res.*, 2018, **144:** 215–225.

[89] TALAPANENI S N, LEE J H, JE S H, *et al*. Chemical blowing approach for ultramicroporous carbon nitride frameworks and their applications in gas and energy storage. *Adv. Funct. Mater.*, 2017, **27(1):** 1604658.

[90] WENG Q, WANG X, WANG X, *et al.* Functionalized hexagonal boron nitride nanomaterials: emerging properties and applications. *Chem. Soc. Rev.*, 2016, **45(14):** 3989–4012.

[91] JIANG X, WENG Q, WANG X, *et al.* Recent progress on fabrications and applications of boron nitride nanomaterials: a review. *J. Mater. Sci. Technol.*, 2015, **31(6):** 589–598.

[92] WANG X, ZHI C, WENG Q, *et al*. Boron nitride nanosheets: novel syntheses and applications in polymeric composites. *J. Phys.: Conf. Ser.*, 2013, **471:** 012003.

[93] LI X, WANG X, ZHANG J, *et al.* Hollow boron nitride nanospheres as boron reservoir for prostate cancer treatment. *Nat. Commun.*, 2017, **8:** 13936.

[94] WENG Q, WANG B, WANG X, *et al.* Highly water-soluble, po-

rous, and biocompatible boron nitrides for anticancer drug delivery. *ACS Nano*, 2014, **8(6):** 6123–6130.

[95] MALEKI M, BEITOLLAHI A, SHOKOUHIMEHR M. Template-free synthesis of porous boron nitride using a single source precursor. *RSC Adv.*, 2015, **5(58):** 46823–46828.

[96] WANG X, PAKDEL A, ZHI C, *et al.* High-yield boron nitride nanosheets from "chemical blowing": towards practical applications in polymer composites. *J. Phys. Condens. Matter*, 2012, **24(31):** 314205.

[97] WENG Q, IDE Y, WANG X, *et al.* Design of BN porous sheets with richly exposed (002) plane edges and their application as TiO_2 visible light sensitizer. *Nano Energy*, 2015, **16:** 19–27.

[98] LEI W, PORTEHAULT D, LIU D, *et al.* Porous boron nitride nanosheets for effective water cleaning. *Nat. Commun.*, 2013, **4(2):** 1777.

[99] LIAN G, ZHANG X, ZHANG S, *et al.* Controlled fabrication of ultrathin-shell BN hollow spheres with excellent performance in hydrogen storage and wastewater treatment. *Energy Environ. Sci.*, 2012, **5(5):** 7072–7080.

[100] WENG Q, WANG X, BANDO Y, *et al.* One-step template-free synthesis of highly porous boron nitride microsponges for hydrogen storage. *Adv. Energy Mater.*, 2014, **4(7):** 1301525.

[101] WENG Q, WANG X, ZHI C, *et al.* Boron nitride porous microbelts for hydrogen storage. *ACS Nano*, 2013, **7(2):** 1558–1565.

[102] XUE Y, DAI P, JIANG X, *et al.* Template-free synthesis of boron nitride foam-like porous monoliths and their high-end applications in water purification. *J. Mater. Chem. A*, 2016, **4(4):** 1469–1478.

[103] NAG A, RAIDONGIA K, HEMBRAM K P S S, *et al.* Graphene analogues of BN: novel synthesis and properties. *ACS Nano*, 2010, **4(3):** 1539–1544.

[104] WU P, ZHU W, CHAO Y, *et al.* A template-free solvent-mediated synthesis of high surface area boron nitride nanosheets for aerobic oxidative desulfurization. *Chem. Commun.*, 2016, **52(1):** 144–147.

[105] CI L, SONG L, JIN C, *et al.* Atomic layers of hybridized boron nitride and graphene domains. *Nat. Mater.*, 2010, **9(5):** 430–435.

[106] LIU S, WANG Z, HAN T, *et al*. Mesoporous magnesium oxide nanosheet electrocatalysts for the detection of lead (II). *ACS Appl. Nano Mater.*, 2019, **2(5):** 2606–2611.

[107] LU K, XU J, ZHANG J, *et al*. General preparation of three-dimensional porous metal oxide foams coated with nitrogen-doped carbon for enhanced lithium storage. *ACS Appl. Mater. Interfaces*, 2016, **8(27):** 17402–17408.

[108] MEZA L R, DAS S, GREER J R. Strong, lightweight, and recoverable three-dimensional ceramic nanolattices. *Science*, 2014, **345(6202):** 1322–1326.

[109] SCHAEDLER T A, JACOBSEN A J, TORRENTS A, *et al*. Ultralight metallic microlattices. *Science*, 2011, **334(6058):** 962–965.

[110] WU Y, YI N, HUANG L, *et al.* Three-dimensionally bonded spongy graphene material with super compressive elasticity and near-zero Poisson's ratio. *Nat. Commun.*, 2015, **6:** 6141.

[111] QIU L, COSKUN M B, TANG Y, *et al.* Ultrafast dynamic piezoresistive response of graphene-based cellular elastomers. *Adv. Mater.*, 2016, **28(1):** 194–200.

[112] JI H, SELLAN D P, PETTES M T, *et al.* Enhanced thermal conductivity of phase change materials with ultrathin-graphite foams for thermal energy storage. *Energy Environ. Sci.*, 2014, **7(3):** 1185–1192.

[113] WANG X, WENG Q, WANG X, *et al.* Biomass-directed synthesis of 20 g high-quality boron nitride nanosheets for thermoconductive polymeric composites. *ACS Nano*, 2013, **8(9):** 9081–9088.

[114] WANG X, PAKDEL A, ZHANG J, *et al.* Large-surface-area BN nanosheets and their utilization in polymeric composites with improved thermal and dielectric properties. *Nanoscale Res. Lett.*, 2012,**7(1):** 662.

[115] XU C, MIAO M, JIANG X, *et al.* Thermal conductive composites reinforced *via* advanced boron nitride nanomaterials. *Compos. Commun.*, 2018, **10:** 103–109.

[116] ZENG X, YAO Y, GONG Z, *et al*. Ice-templated assembly strategy to construct 3D boron nitride nanosheet networks in polymer composites for thermal conductivity improvement. *Small*, 2015, **11(46):** 6205–6213.

[117] XUE Y, DAI P, ZHOU M, *et al*. Multifunctional superelastic foam-like boron nitride nanotubular cellular-network architectures. *ACS Nano*, 2017, **11(1):** 558–568.

[118] TIAN Z, SUN J, WANG S, *et al.* A thermal interface material based on foam-templated three-dimensional hierarchical porous boron nitride. *J. Mater. Chem. A*, 2018, **6(36):** 17540–17547.

[119] NARASIMMAN R, VIJAYAN S, PRABHAKARAN K. Carbon particle induced foaming of molten sucrose for the preparation of carbon foams. *Mater. Sci. Eng. B*, 2014, **189:** 82–89.

[120] SUN Q, LI Z, SEARLES D J, *et al*. Charge-controlled switchable CO_2 capture on boron nitride nanomaterials. *J. Am. Chem. Soc.*, 2013, **135(22):** 8246–8253.

[121] WENG Q, WANG X, WANG X, *et al.* Preparation and hydrogen sorption performances of BCNO porous microbelts with ultra-narrow and tunable pore widths. *Chem. Asian J.*, 2013, **8(12):** 2936–2939.

[122] JIA H, LI J, LIU Z, *et al.* Three-dimensional carbon boron nitrides with a broken, hollow, spherical shell for water treatment. *RSC Adv.*, 2016, **6(82):** 78252–78256.

[123] LI J, HUANG Y, LIU Z, *et al.* Chemical activation of boron nitride fibers for improved cationic dye removal performance. *J. Mater. Chem. A*, 2015, **3(15):** 8185–8193.

[124] LIN J, XU L, HUANG Y, *et al.* Ultrafine porous boron nitride nanofibers synthesized *via* a freeze-drying and pyrolysis process and their adsorption properties. *RSC Adv.*, 2016, **6(2):** 1253–1259.

[125] ZHANG X, LIAN G, ZHANG S, *et al.* Boron nitride nanocarpets: controllable synthesis and their adsorption performance to organic pollutants. *CrystEngComm*, 2012, **14:** 4670–4676.

[126] CHANDKIRAM G CHANDRA S T, SUJIN J. Synthesis of low-density, carbon-doped, porous hexagonal boron nitride solids. *ACS Nano*, 2015, **9(12):** 12088–12095.

[127] LIN J, YUAN X, LI G *et al.* Self-assembly of porous boron nitride microfibers into ultralight multifunctional foams of large sizes. *ACS Appl. Mater. Interfaces*, 2017, **9(51):** 44732–44739.

[128] WU C, WANG B, WANG Y. One-step fabrication of boron nitride fibers networks. *Ceram. Int.*, 2018, **44(5):** 5385–5391.

[129] CHOI B G, YANG M H, HONG W H, *et al.* 3D macroporous graphene frameworks for supercapacitors with high energy and power densities. *ACS Nano*, 2012, **6(5):** 4020–4028.

[130] CHEN P, YANG J, LI S, *et al.* Hydrothermal synthesis of macroscopic nitrogen-doped graphene hydrogels for ultrafast supercapacitor. *Nano Energy*, 2013, **2(2):** 249–256.

[131] YANG X, ZHU J, QIU L, *et al.* Bioinspired effective prevention of restacking in multilayered graphene films: towards the next generation of high-performance supercapacitors. *Adv. Mater.*, 2011, **23(25):** 2833–2838.

[132] YANG X, CHENG C, WANG Y, *et al.* Liquid-mediated dense integration of graphene materials for compact capacitive energy storage. *Science*, 2013, **341(6145):** 534–537.

[133] DONG X, XU H, WANG X, *et al.* 3D Graphene-cobalt oxide electrode for high-performance supercapacitor and enzymeless glucose detection. *ACS Nano*, 2012, **6(4):** 3206–3213.

[134] KIM B, YANG G, PARK M, *et al.* Three-dimensional graphene foam-based transparent conductive electrodes in GaN-based blue light-emitting diodes. *Appl. Phys. Lett.*, 2013, **102(16):** 161902.

[135] CHEN Z, XU C, MA C, *et al.* Lightweight and flexible graphene foam composites for high-performance electromagnetic interference shielding. *Adv. Mater.*, 2013, **25(9):** 1296–1300.